UNDERSTANDING THE LIMITS OF THERMAL RUNAWAY IN LITHIUM-ION BATTERY SYSTEMS

John C. Hewson (jchewso@sandia.gov, 1-505-284-9210) Sandia National Laboratories Albuquerque, NM 87185-0836 USA

ABSTRACT

Stored energy in batteries can lead to thermal runaway and ignition if the cell components are heated. The chemical processes associated with the early stages of heating in lithium-ion batteries are reviewed, and a set of reactions representing these processes is employed with a lumped model of thermal evolution to examine some theoretical limits on ignition. Different cathode materials have different thermal runaway temperatures and this leads to inherent differences in the safety of these batteries. The parameter space associated with heating of the lumped cell model for two cathode materials is explored to explain the significance of the various processes. The heat release associated with processes occurring at lower temperatures is modest and slow relative to many fire-related processes. Reactions between the cathode and the electrolyte are more strongly exothermic and temperature dependent so that ignition can be most closely associated with the thermal runaway of these reactions.

INTRODUCTION

As the importance of electrical energy storage increases, the hazards associated with unintentional release of that energy must be addressed. Internally, batteries typically have both fuel and oxidizer, making them a premixed system subject to thermal runaway. Experience with other forms thermal runaway has led to continually improving best practices, but less experience exists with batteries for large-scale energy storage. Improved understanding of the best approaches is needed to maximize safety through a combination of testing, careful experimentation to understand phenomena and the development of modeling approaches that aid in interpreting and extending measured phenomena. The current industry and regulatory approach to studying battery failures at the system level relies on testing. As system sizes increase there will be requirements to analyze and test increasingly expensive systems. To date, there are no system-level simulation tools that adequately predict the range of processes that occur during thermal runaway in batteries. This work seeks to explore the parameter space using models to better design test programs in order to minimize the costs associated with larger scale systems.

Lithium-ion batteries are particularly desirable for energy storage applications because of their high energy and power density. Within lithium-ion batteries a series of exothermic and gas-generating reactions can take place as temperatures rise or as the battery is otherwise put into an unstable state (overcharging is an alternate unstable state). Some of these reactions are related to the internal battery chemistry while others involve the combustion in air of battery components including hydrocarbon based liquid electrolytes and plastic packaging.

Some of the reactions that are important at the lowest temperatures are those internal to the battery. These include reactions associated with the decomposition of the electrolyte and its reaction with lithium from the anode. At slightly higher temperatures, reactions of the cathode with electrolytes become important. The rate of exothermic reaction at these temperatures is relatively low, and it is possible to consider balances between the heat release and its dissipation leading to an avoidance of thermal runaway. In this work we discuss the balance in between heat release and dissipation using models of heat release for the various materials. These models take advantage of tests and measurements of battery abuse scenarios in the literature, and allowing us to map the boundaries

between a partial and complete thermal runaway. The rates of reaction in this low temperature range are also strongly dependent on the battery materials, and new materials are an active area of development. We discuss the sensitivity of various ignition scenarios to changes that might come from material changes through the consideration of models for two different cathode materials.

FORMULATION

In this paper a simplified thermal model is employed. Cells are typically assumed to be nearly homogeneous in temperature with external and inter-cell heat transfer being the limiting process. Masses and heat capacities can be associated with cells and layers of insulting or conducting materials between the cells. Within reactive cells, the evolution of the reactive components will be tracked through their progress variables, Y_i , a normalized mass concentration, that evolve according to the simple homogeneous conservation equation

$$\frac{dY_i}{dt} = -A_i f_i(\mathbf{Y}) \exp(-E_i / RT) \tag{1}$$

where A_i and E_i are the pre-exponential coefficient and activation energy associated with an assumed single reaction consuming the reactant i. The various reactions and reactants considered are detailed in the following section. The dependence of the reaction rate on the progress variables of the various species is given in a general form as $f_i(\mathbf{Y})$ as given below. Conservation of energy is expressed here as

$$\rho c_{p} \frac{dT}{dt} = \sum_{i} A_{i} f_{i} (\mathbf{Y}) \rho_{i} \Delta H_{i} \exp(-E_{i}/RT) + h_{eff} (S/V) (T_{\infty} - T) + \varepsilon \sigma (S/V) (T_{\infty}^{4} - T^{4}) + Q_{s}$$
(2)

where reactions over all species i contribute according to the reaction enthalpy per unit mass for that species consumption, ΔH_i and its mass per unit volume, ρ_i . External heat flux is characterized by a heat transfer coefficient, h_{eff} , and a surface emissivity, ε , both acting over a surface-to-volume ratio, S/V. The environment temperature is T_{∞} . In this work, we will examine a single bulk temperature within the cells.

We also use a correction to the heat transfer coefficient that can be used to account for small temperature gradients associated with the boundary layers by comparing the basic unsteady and steady ignition theories of Frank-Kamenetskii and Semenov as discussed in the next paragraph.

Cells can be isolated and exposed to the environment, but they are likely to be encased in some insulation or with highly conductive connections to the surroundings. In addition there will be an internal boundary layer within the cell that reflects temperature non-uniformity within the cell. Combinations of heat conduction pathways acting in series are additive as in

$$\frac{1}{h_{eff}} = \frac{1}{h_c} + \frac{1}{h_{in}} + \frac{1}{h_{bl}} \tag{3}$$

where the heat transfer across the cell, h_c , across an insulation layer, h_{in} , and across a boundary layer, h_{bl} , can all be combined into an effective heat transfer coefficient, h_{eff} . Frank-Kamenetskii gives an effective heat transfer coefficient across a cell with nearly homogeneous temperature in terms of the critical Damköhler number, δ_{cr} . In terms of a Nusselt number this is [1]

$$Nu_{c} = \frac{h_{c}d}{\lambda} = e^{1} \left[2.0 + \left(\frac{\pi d}{4L} \right)^{2} \right]$$
 (4)

for a cylinder of length L, diameter d and thermal conductivity λ . We note that for an infinite planar cell that might approximate the heat transfer characteristics for a pouch cell, $Nu_c = 4.8$; this is close enough to that for a cylinder, especially with a correction for finite pouch size, that the analysis of the cylindrical cell dimensions can be considered for the present purposes. The expression in Eq. (4) is used in all calculations presented here along with other specified external heat transfer coefficients.

CHEMISTRY AND PHYSICS OF CELL THERMAL RUNAWAY

Batteries are composed of an anode and cathode separated by an electrolyte through which ions but not electrons flow, the electrons being required to perform work by flowing through whatever

circuit the battery is attached to. The energy stored in batteries comes from the change in the Gibbs free energy between the charged and discharged state of the anode and cathode. For a standard lithium-ion chemistry, this overall reaction can be written

$$C_6 \text{Li} + \text{CoO}_2 \rightarrow C_6 + \text{LiCoO}_2 \quad \Delta G \approx 400 \text{ kJ mol}^{-1} \text{ Li}.$$
 (5)

Considering the mass of just the active materials, this leads to a theoretical energy density of approximately 1.5 MJ kg⁻¹, but a practical battery including packaging would have an energy density closer to 0.5 MJ kg⁻¹ [2]. While this energy density is small relative to many fire sources, the battery also contains flammable electrolyte and polymers with additional energy content as discussed in Ref. [3].

To attain these energy densities the anode and cathode materials are strongly reactive and this leads to the strong potential for thermal runaway. Since lithium and lithiated-carbon are too reactive to contact water, alkyl carbonates are typically employed as electrolytes. These are flammable as discussed elsewhere [3], and a significant hazard is associated with thermal runaway leading to cell pressurization and the venting of a flammable electrolyte in aerosolized form. This paper addresses the processes that lead up to this venting, the ignition process, and does not address the actual alkyl carbonate combustion in air. Though they are less reactive than aqueous solutions, the alkyl carbonates will react both with lithium and with the cathode material as described in the next paragraphs, and it is these processes that lead to thermal runaway.

During normal operation the lithium in the anode reacts with the alkyl carbonates and forms a passivation layer referred to as the solid-electrolyte interface (SEI) layer. This SEI layer is thought to contain metastable salts of lithium alkyl carbonates that have been associated with exothermic decomposition at temperatures in the vicinity of 90 to 120 C in a reaction that might be representatively written [4]

$$(CH_2OCO_2Li)_2 \rightarrow Li_2CO_3 + CH_4 + CO_2 + CO$$
 (6)

though the gaseous products may vary. As temperatures rise, lithium in the anode will continue to react with the electrolyte resulting in the formation and consumption of the reactant in Reaction (6). This reaction is inhibited by the buildup of the SEI passivation layer that is represented by Li₂CO₃ in its more thermally stable form, and this passivation layer limits this otherwise strongly exothermic process. These two reactions were measured and modeled by Dahn and Richards [5, 6] and are included in Table 1 as the SEI decomposition step and the anode-electrolyte step. The electrolyte is also known to react with the salts that provide conducting ions, typically LiPF₆ that decomposes itself [7], and this reaction is given in Table 1 as the electrolyte decomposition step; this reaction primarily occurs at temperatures above 200 C.

In addition to being reduced by lithium, the alkyl carbonates can be oxidized by the cathode materials, typically metal oxides. At elevated temperatures these metal oxides will undergo disproportionation reactions as, for example,

$$CoO_2 \rightarrow \frac{1}{3}Co_3O_4 + \frac{1}{3}O_2 \quad \text{or} \quad Mn_2O_4 \rightarrow Mn_2O_3 + \frac{1}{2}O_2$$
 (7)

where the resulting oxygen can oxidize the electrolyte. The reaction for the CoO_2 cathode is observed to occur for temperatures above 180 C [8] while the Mn_2O_4 cathode primarily reacts above 220 C [9]; this temperature difference will be observed to be important in the potential stability of cells as described in the next section. It is highly unlikely that these reactions go to completion before the cell undergoes strong venting or disassembly, so that the heat release associated with these processes is highly uncertain. Reactions for these two cathode materials are provided in Table 1 with estimates for the rates and the exothermicity that are expected to be less certain than the other rates because measurements at these temperatures are contaminated by other processes.

Table 1. Reaction rate description. For simplicity and consistency with existing literature, the reactants are expressed in normalized progress variables instead of strict mass fractions or concentrations.

Reaction description	Y_i	Initial value	$f_i\left(\mathbf{Y}\right)$	$A_i \ [ext{s}^{ ext{-}1}]$	E_i [kJ mol ⁻¹]	ΔH_i [kJ mol ⁻¹]	Ref.
Metastable SEI decomposition	$Y_{ m SEI}$	0.15	$Y_{ m SEI}$	1.67e15	135	257	[5, 6]
Anode-electrolyte reaction	$Y_{\rm C6Li}$	0.45	$Y_{\text{C6Li}} e^{-z/0.33}$ (a)	1.67e6	77.2	1714	[5, 6]
Electrolyte decomposition	$Y_{\rm Elyte}$	1.0	$Y_{ m Elyte}$	5.1e25	274	155	[9]
CoO ₂ -electrolyte reaction	Y_{CoO2}	0.96	$Y_{\text{CoO2}}(1-Y_{\text{CoO2}})$	6.67e11	122	314	[8]
Mn ₂ O ₄ -electrolyte reaction	$Y_{ m Mn2O4}$	0.96	$Y_{ m Mn2O4}$	1.4e13	150	450	[9]

(a) The source term for the anode-electrolyte is reduced by the passivation layer thickness according to $f_{C_0Li}(\mathbf{Y}) = Y_{C_0Li} \exp(-z/0.033)$ where $z = 0.033 + \left(Y_{C_0Li,0} - Y_{C_0Li}\right) + \left(Y_{SEI,0} - Y_{SEI}\right)$ is the contribution of the metastable SEI decomposition and anode-cathode reaction to this passivation layer thickness in addition to its initial thickness which is estimated at 0.033 [5, 6].

Table 2. Parameters for evolution of Eqs. (1) and (2) are representative values taken from [10].

Parameter	value	Parameter	value	Parameter	value
S/V	48.4 m ⁻¹	λ	0.034 W m ⁻¹ K ⁻¹	$ ho_{ m C6Li}$	610 kg m ⁻³
	2.79e6 J m ⁻³	3	0.8	$ ho_{ ext{Elyte}}$	1221 kg m ⁻³
h_{bl}	7.17 W m ⁻² K ⁻¹	σ	5.67e-8 W m ⁻² K ⁻⁴	$ ho_{\mathrm{CoO2}}$	407 kg m^{-3}
d	0.018 m	L	0.065 m	$ ho_{ m Mn2O4}$	407 kg m^{-3}

SIMULATIONS OF THERMAL RUNAWAY

In this section we simulate thermal abuse scenarios and discuss the thermal aspects of the cell evolution in these cases. We discuss the overheating of a battery in a high temperature environment and the potential that will lead to strongly exothermic thermal runaway; here we define strongly exothermic as runaway that significantly involves the cathode oxidation of the electrolyte. All simulations are carried out using nominal properties indicated in Table 2 that are representative of 18650 size cells except as noted. The parameters given here, while taken from other literature studies, do not exactly reproduce all measurements and further development of this parameter set is needed.

The configuration for simulations is referred to as an oven test, and it simulates the response to elevated environment temperatures. These tests define a fixed environmental temperature, T_{∞} , with both convection and radiative heat transfer to/from a cell initially at ambient temperature as per Eq. (2). These simulations are relevant to fire environments as T_{∞} can be related to the fire environment. Figure 1 shows the temperature evolution and it's net source term at two oven temperatures for both cathode materials given in Table 1, CoO_2 and Mn_2O_4 . Because of the strong activation energies associated with the various exothermic processes and especially the cathode decomposition, the environment temperature and the rate constant for the limiting reaction are the most important factors in determining the degree of thermal runaway and heating that occur. The cathode material is identified here as the limiting reaction, and two cathode materials are considered to investigate the role of material choices in thermal runaway. The cases at 150 C show that the Mn_2O_4 cathode does not experience significant heat release while the CoO_2 cathode does undergo full thermal runaway.

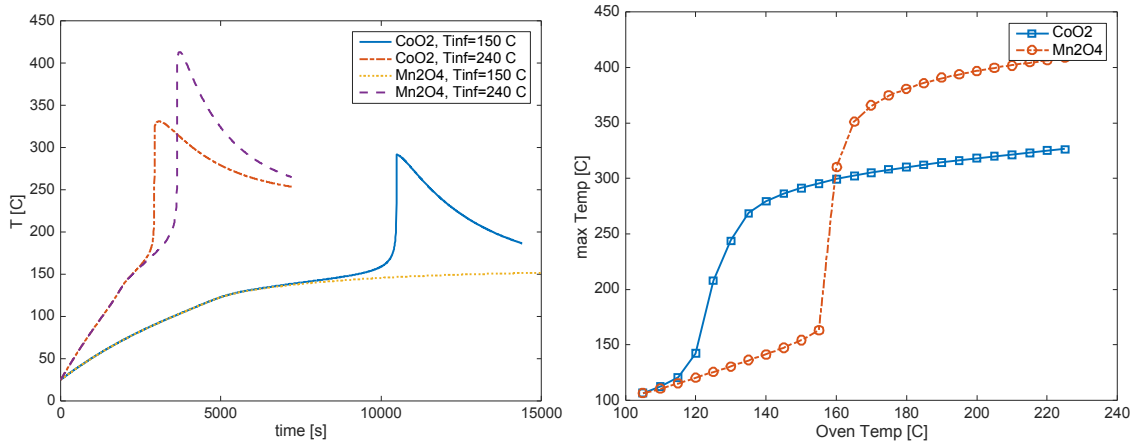


Figure 1. The temperature evolution for four cases, two temperatures with each cathode. The right panel shows the maximum temperature observed as a function of the environment (oven) temperature.

The thermal runaway temperature for each cathode material is evident in right panel of Figure 1 where it can be seen that the difference in the cathode chemistry leads to thermal runaway occurring around 120 C and 160 C for CoO₂ and Mn₂O₄ cathodes for this particular set of conditions. This is related to the temperature at which the disproportionation reactions listed in Eq. (7) occur as represented by the rate constants for the cathode reaction. This is clear in Figure 2 where the evolution of the various state variables are shown for the two cases at 150 C. For the CoO₂ cathode case the cathode material is fully consumed while only a small fraction of the cathode reacts for the Mn_2O_4 cathode at this same T_{∞} . Additional phenomena are evident in Figure 2. First, the SEI passivation layer (labeled 'thickness' in Figure 2) inhibits the reaction between the anode, C₆Li, and the electrolyte, so that this reaction is only significant at higher temperatures that are reached through the cathode decomposition. That is, the significant potential heat release associated with the anodeelectrolyte reaction is predicted to play a small role because of the passivation layer; the estimated temperature rise associated with this reaction is only on the order of 10 C. Second, the heat release associated with electrolyte decomposition is insignificant until the temperatures where the cathode reaction leads to thermal runaway. The reaction between the anode and the electrolyte can provide similar contributions to heating in this temperature range.

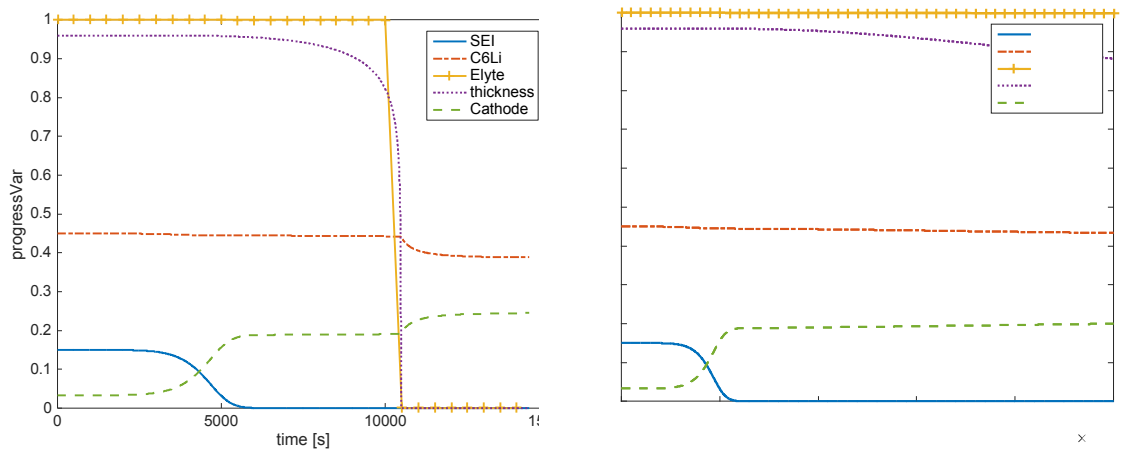


Figure 2. The evolution of the progress variables for each active component in the evolution of (left) CoO_2 and (right) Mn_2O_4 at 150 C. For the Mn_2O_4 cathode the cathode material does not react fast enough for the cell to runaway.

In Figure 3 the contribution of the chemical source term to the rate of heating is plotted for the four cases shown in Figure 1; there are two features of note. First, the peak in heat release around 120 to 130 C is associated with the SEI decomposition. It is important to note that the rate of chemical heat release is larger for the higher environmental temperature; this occurs because the external heat

transfer also contributes significantly to the rate of heating leading to faster kinetic rates for these reactions. For faster rates of heating the degree of consumption of the reactants at a given temperature is less for the larger T_{∞} , as shown in the right panel of Figure 3. This allows a larger chemical heat release at higher temperatures that can provide a small but nonnegligible contribution to heating to those temperatures where the cathode chemistry is important. That is, while the environment temperature is of primary importance, the rate of heating can also play a role through the finite rate of reactant consumption. We note, however, that a simple balance between heat transfer and cathode-electrolyte reaction rate, the Semenov ignition criterion, suggests that for the activation energies relevant here, a factor of two change in the heat transfer rate itself is of minor importance: the fractional change in the critical ignition temperature per fractional change in the heat transfer coefficient, $d \ln T_{ig} / d \ln h$, is given by an order unity Zel'dovich number, $\Delta T_{ig} \approx R T_{ig}^2 / E_{ce}$, which is small since the activation energy associated with the cathode reaction is large.

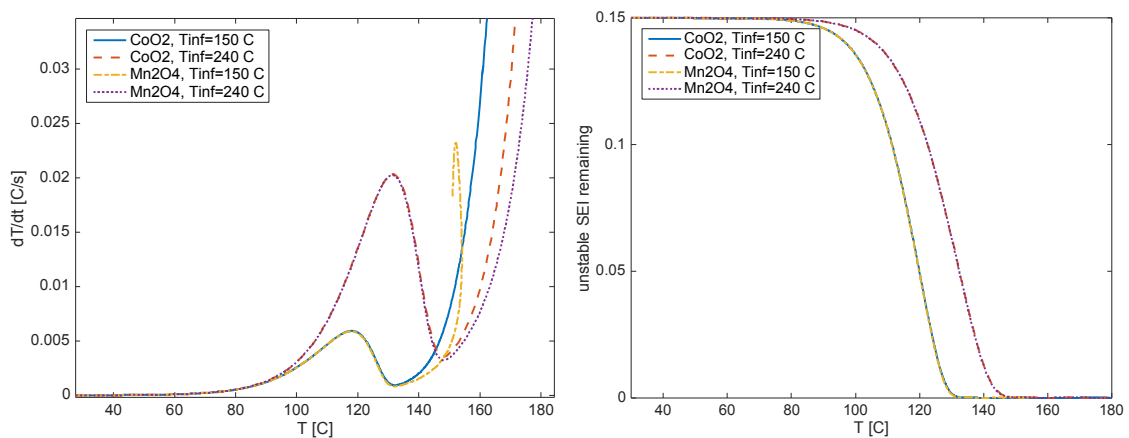


Figure 3. The temperature source term from chemical reactions (in temperature rate of change units) for the four cases shown in Figure 1 (left) and the fraction of electrolyte remaining as a function of temperature (right).

SUMMARY AND CONCLUSIONS

This work describes exothermic processes that can lead to thermal runaway in lithium-ion batteries. The processes considered are internal to the cells and occur when the cell is heated by some source. Reactions are predominantly associated with reactions between the electrolyte and either the anode or cathode; this includes reactions of the anode SEI passivation layer. Reactions representative of these internal processes are taken from the literature and used in a lumped thermal model to understand the limits of thermal runaway and ignition.

The oven test with a prescribed elevated environmental temperature is used as a prototypical test condition that could also represent fire environments. For this configuration, the limit of ignition is determined by thermal runaway of the cathode-electrolyte reaction. The thermal-runaway temperature of this reaction depends on the cathode material, and this leads to a difference in the potential hazards for different battery chemistries. A number of processes occur at lower temperatures during the heating process; noteworthy among these processes is the decomposition of the metastable components of the anode SEI passivation layer. Depending on the rate of heating, these lower-temperature processes may continue to release heat as the critical temperature for the cathode-electrolyte reaction is approached so that the transient rate of heating might be relevant in addition to the environment temperature, though these are related in the present configuration.

ACKNOWLEDGEMENTS

Sandia National Laboratories is a multi-program laboratory operated by Sandia Corporation, a Lockheed Martin Company for the United States Department of Energy's National Nuclear Security Administration under contract DE-AC04-94AL85000. The authors gratefully acknowledge funding from the Department of Energy, Office of Electricity's Energy Storage Program. The authors would like to thank Dr. Imre Gyuk for his support and guidance of this effort.

REFERENCES

- [1] D. A. Frank-Kamenetskii, Diffusion and Heat Exchange in Chemical Kinetics, 2nd ed.: Plenum, 1969.
- [2] D. Linden, ed., *Handbook of Batteries*: McGraw-Hill, 2002.
- [3] J. C. Hewson and S. P. Domino, "Thermal runaway of lithium-ion batteries and hazards of abnormal thermal environments," 114TF-0222, presented at the Meeting of the United States Section of the Combustion Institute, Cincinnati, 2015.
- [4] D. Aurbach, B. Markovsky, I. Weissman, E. Levi, and Y. Ein-Eli, "On the correlation between surface chemistry and performance of graphite negative electrodes for Li ion batteries," *Electrochimica Acta*, vol. 45, pp. 67-86, 1999.
- [5] M. N. Richard and J. R. Dahn, "Accelerating rate calorimetry study on the thermal stability of lithium intercalated graphite in electrolyte I. Experimental," *Journal of the Electrochemical Society*, vol. 146, pp. 2068-2077, Jun 1999.
- [6] M. N. Richard and J. R. Dahn, "Accelerating rate calorimetry study on the thermal stability of lithium intercalated graphite in electrolyte II. Modeling the results and predicting differential scanning calorimeter curves," *Journal of the Electrochemical Society*, vol. 146, pp. 2078-2084, Jun 1999.
- [7] S. E. Sloop, J. K. Pugh, S. Wang, J. B. Kerr, and K. Kinoshita, "Chemical reactivity of PF5 and LiPF6 in ethylene carbonate/dimethyl carbonate solutions," *Electrochemical and Solid State Letters*, vol. 4, pp. A42-A44, Apr 2001.
- [8] D. D. MacNeil, L. Christensen, J. Landucci, J. M. Paulsen, and J. R. Dahn, "An autocatalytic mechanism for the reaction of LixCoO2 in electrolyte at elevated temperature," *Journal of the Electrochemical Society*, vol. 147, pp. 970-979, Mar 2000.
- [9] R. Spotnitz and J. Franklin, "Abuse behavior of high-power, lithium-ion cells," *Journal of Power Sources*, vol. 113, pp. 81-100, Jan 1 2003.
- [10] T. D. Hatchard, D. D. MacNeil, A. Basu, and J. R. Dahn, "Thermal model of cylindrical and prismatic lithium-ion cells," *Journal of the Electrochemical Society*, vol. 148, pp. A755-A761, Jul 2001.